The LINNEAN SOCIETY of London BIOLOGICAL Journal of the Linnean Society

Biological Journal of the Linnean Society, 2013, **110**, 852–865. With 5 figures

Phylogeography of the Trans-Volcanic bunchgrass lizard (*Sceloporus bicanthalis*) across the highlands of south-eastern Mexico

ADAM D. LEACHÉ[1]*, JULIA A. PALACIOS[2], VLADIMIR N. MININ[2] and ROBERT W. BRYSON Jr[1]

[1]*Department of Biology and Burke Museum of Natural History and Culture, University of Washington, Box 351800, Seattle, WA 98195, USA*
[2]*Department of Statistics, University of Washington, Seattle, WA 98195-4322, USA*

Received 15 May 2013; revised 7 July 2013; accepted for publication 7 July 2013

We quantify the population divergence processes that shaped population genetic structure in the Trans-Volcanic bunchgrass lizard (*Sceloporus bicanthalis*) across the highlands of south-eastern Mexico. Multilocus genetic data from nine nuclear loci and mitochondrial (mt)DNA were used to estimate the population divergence history for 47 samples of *S. bicanthalis*. Bayesian clustering methods partitioned *S. bicanthalis* into three populations: (1) a southern population in Oaxaca and southern Puebla; (2) a population in western Puebla; and (3) a northern population with a broad distribution across Hidalgo, Puebla, and Veracruz. The multilocus nuclear data and mtDNA both supported a Late Pleistocene increase in effective population size, and the nuclear data revealed low levels of unidirectional gene flow from the widespread northern population into the southern and western populations. Populations of *S. bicanthalis* experienced different demographic histories during the Pleistocene, and phylogeographical patterns were similar to those observed in many co-distributed highland taxa. Although we recommend continuing to recognize *S. bicanthalis* as a single species, future research on the evolution of viviparity could gain novel insights by contrasting physiological and genomic patterns among the different populations located across the highlands of south-eastern Mexico. *Biological Journal of the Linnean Society*, 2013, **110**, 852–865.

ADDITIONAL KEYWORDS: biogeography – coalescence – divergence – gene flow – Phrynosomatidae – Pleistocene – skyline plot – species delimitation.

INTRODUCTION

Recent studies on the evolution of Mexican highland biotas suggest that dynamic geological and climatic processes have differentially structured phylogeographical diversity among co-distributed highland taxa (Bryson, García-Vázquez & Riddle, 2012; Bryson & Riddle, 2012). Pre-Pleistocene events heavily impacted genetic diversification in some montane taxa (McCormack *et al*., 2008; Bryson *et al*., 2012), whereas Quaternary climate change appeared to trigger diversification in others (Bryson *et al*., 2011a; Parra-Olea *et al*., 2012). However, a clear pattern that has emerged from these studies is that cryptic diversity across the Mexican highlands is high, and multilocus studies are needed to better understand population divergence processes that have shaped population genetic structure.

Sceloporus bicanthalis is a small (mean snout–vent length of approximately 45 mm) terrestrial lizard that is closely associated with high-elevation bunchgrass habitats across the highlands of south-eastern Mexico. The monophyly of *S. bicanthalis*, and that of the *scalaris* species group to which it belongs, are well established (Mink & Sites, 1996; Benabib, Kjer & Sites, 1997; Creer, Kjer & Simmons, 1997; Bryson *et al*., 2012). However, the number of species contained within the *scalaris* group is unclear, and a recent species delimitation study suggests that the

*Corresponding author. E-mail: leache@uw.edu

group contains up to 12 species (Grummer, Bryson & Reeder, 2013). Although most species in the group are oviparous (i.e. egg-laying), two species appear to have independently evolved viviparity (live birth), including *Sceloporus goldmani* and *S. bicanthalis* (Benabib *et al*., 1997). *Sceloporus goldmani* is considered to be extinct because recent field surveys have failed to detect this species at multiple historical collecting localities (Sinervo *et al*., 2010; Bryson *et al*., 2012). *Sceloporus bicanthalis*, on the other hand, is widely distributed across high elevations in south-eastern Mexico and has become a model for studies of viviparity and placentation (Guillette, 1982; Méndez de la Cruz, Villagrán-Santa Cruz & Andrews, 1998; Andrews *et al*., 1999; Andrews, 2000; Rodríguez-Romero *et al*., 2004). The evolution of viviparity in *S. bicanthalis* could be an outcome of their geographical distribution at high-elevation regions; according to the cold-climate model (Mell, 1929; Tinkle & Gibbons, 1977; Shine, 1985; Andrews, 2000), constraints on the thermal biology of embryos can drive the evolution of viviparity because egg retention and viviparity can compensate for the negative effects of low temperatures on embryonic developmental rates that lizards experience at high elevation.

In the present study, we investigated the population divergence processes that have shaped population genetic structure in *S. bicanthalis* across the highland regions of south-eastern Mexico. Previous studies utilizing mitochondrial (mt)DNA have revealed phylogeographical structure within *S. bicanthalis* (Benabib *et al*., 1997; Bryson *et al*., 2012), although whether mtDNA clades correspond to actual interbreeding populations or to cryptic species remains untested. We used multilocus nuclear data and mtDNA to estimate the population divergence history within *S. bicanthalis*. Bayesian population structure analyses were used to infer the number of populations and the assignment of samples to populations. The inferred population structure is assumed in subsequent inferences of coalescent-based population relationships, effective population size trajectories, and genetic connectivity. We estimated a time-calibrated species tree to gain insight into the timing of population divergence across south-eastern Mexico, and also to provide a temporal component to the effective population size trajectories. Finally, we tested species delimitation models for *S. bicanthalis* that include one, two, and three species. We base our phylogeographical inferences largely on our multilocus nuclear data. Independently segregating genes can each have a unique history that is shaped by population demography, life history, genetic drift, selection, and introgression, and so multilocus data are thus valuable for investigating phylogeography (Edwards & Bensch, 2009).

MATERIAL AND METHODS

Sampling

A total of 47 specimens of *S. bicanthalis* were collected from ten localities across their distribution in south-eastern Mexico (Fig. 1) along the southern Sierra Madre Oriental, eastern Trans-Mexican Volcanic Belt, and northern Sierra Madre del Sur. *Sceloporus subniger* was included to root phylogenetic trees when necessary. Specific localities and specimen voucher data are provided in the Appendix.

Genetic data

Genomic DNA was extracted from liver, toe clips, and tail clips using Qiagen DNeasy extraction kits (Qiagen Inc.). Nine nuclear loci and one mitochondrial gene were sequenced (Table 1). A polymerase chain reaction (PCR) was performed: 20 ng of genomic DNA were mixed in a 20-μL reaction containing 1.25 mM $MgCl_2$, 1 × Standard Taq (Mg-free) Reaction Buffer (New England Biolabs), 0.4 mM dNTPs, and 0.1 U of NEB Taq DNA polymerase. PCR amplicons were visualized on a 1% TAE agarose gel stained with GelStar (Lonza Group; 0.5 μL per 100 mL). We used touchdown PCR conditions that included an initial denaturation at 94 °C for 1 min, followed by five cycles of 94 °C, 61 °C, and 68 °C, all for 30 s; another five cycles of 94 °C, 59 °C, and 68 °C, all for 30 s; a third round of five cycles of 94 °C, 57 °C, and 68 °C, all at 30 s; and a final 25 cycles of 94 °C at 30 s, 50 °C at 30 s, and 68 °C at 90 s. Excess primers and dNTPs were removed from 10 μL of PCR product with a mixture of 0.3 U of NEB shrimp alkaline phosphatase and 3 U of NEB exonuclease 1 in a 30-min incubation at 37 °C and 15 m at 80 °C. Cycle sequencing of PCR products was accomplished using Big Dye Terminator, version 3.1 Cycle (Applied Biosystems). Reaction products were cleaned using Sephadex G-50 fine (GE Healthcare) based gel filtration in EdgeBio 96-well filter plates. Sequencing (both directions) was performed on an ABI 3730 capillary DNA sequencer. Base calls were checked and contiguous sequences aligned in SEQUENCHER, version 4.9 (Gene Codes). Heterozygous sites were assigned IUPAC standard ambiguity codes and missing sites were coded as '?'.

We used PHASE, version 2.1.1 (Stephens, Smith & Donnelly, 2001; Stephens & Donnelly, 2003) to infer which combinations of alleles were present on each of the two chromosomes for the nuclear genes. Two phased datasets were retained for subsequent analysis, including one with the 'best' phase calls and a second that only retained the samples with ≥ 95% phase confidence.

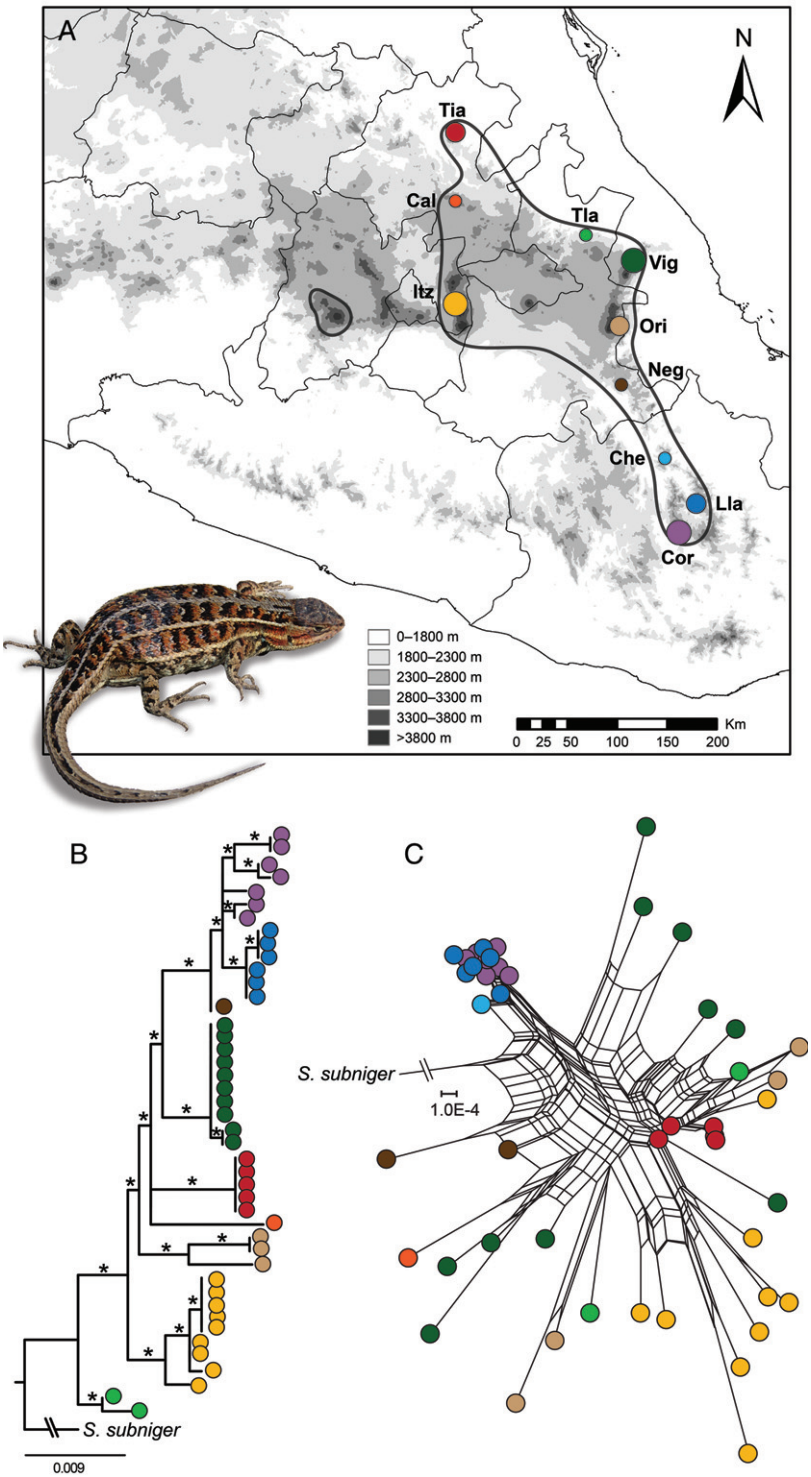

Figure 1. A, approximate distribution of *Sceloporus bicanthalis* (thick grey line) across the mountains of south-eastern Mexico. Colour-coded circles denote sampled localities, with circle sizes proportional to sample size (1–3, 4–6, and 7–10; see also Appendix). B, mitochondrial gene tree estimated using maximum likelihood. Nodes with bootstrap values ≥ 70% and/or Bayesian posterior probability values ≥ 0.95 are marked with an asterisk. C, multilocus network constructed from the nine nuclear loci using the program POFAD. Cal, Calicanto; Tia, Tianguistengo; Che, Cumbre Cerro del Cheve; Cor, Cerro Corral del Piedra; Lla, Llano de las Flores; Itz, Volcán Iztaccihuatl; Neg, Sierra Negra; Tla, Tlatlauquitepec; Ori, Pico de Orizaba; Vig, Las Vigas.

Table 1. Summary of nuclear and mitochondrial gene variation in *Sceloporus bicanthalis*

Locus	Type	Source	Size (bp)	Samples	95% samples	Variable sites	Alleles	H_O/H_E	HWE *P*-value	Model
BDNF	Nuclear	Leaché & McGuire (2006)	685	44	44	6	7	0.20/0.19	1.00	JC
EXPH5	Nuclear	Portik *et al.* (2012)	720	45	33	23	25	0.57/0.82	0.00	F81 + I
KIAA	Nuclear	Alföldi *et al.* (2011)	713	44	40	14	16	0.44/0.82	0.00	HKY
NKTR	Nuclear	Townsend *et al.* (2011)	547	44	43	9	9	0.46/0.70	0.00	HKY
NOS1	Nuclear	Grummer *et al.* (2013)	573	45	45	6	6	0.11/0.63	0.00	HKY
PNN	Nuclear	Townsend *et al.* (2008)	853	37	37	9	12	0.35/0.71	0.00	F81
R35	Nuclear	Leaché (2009)	619	44	42	12	12	0.41/0.52	0.03	K80
RAG1	Nuclear	Leaché & McGuire (2006)	958	43	31	20	19	0.51/0.76	0.00	HKY
SOCS5	Nuclear	Alföldi *et al.* (2011)	395	47	47	1	2	0.25/0.36	0.08	JC
ND1	Mitochondrial	Leaché & Reeder (2002)	972	44	–	67	–	–	–	HKY + Γ

Columns show the locus name, primer source, size in base pairs, number of samples, number of samples with ≥ 95% phase confidence, number of variable sites, number of alleles, mean heterozygosity (observed/expected) across all *S. bicanthalis*, Hardy–Weinberg Exact (HWE) test *P*-values, and nucleotide substitution model (includes outgroup *S. subniger*).

Summary statistics

For each locus, we calculated basic measures of sequence variability, including the number of variable sites, the number of alleles, and the observed heterozygosity as the proportion of heterozygotes in the sample. We compared the observed heterozygosities with the expected Hardy–Weinberg heterozygosities. Discrepancy between observed and expected heterozygosities might be attributable to forces such as inbreeding or mixing of previously isolated populations (Hedrick, 2011). We performed the exact test of Hardy–Weinberg proportion for multiple alleles (Guo & Thompson, 1992). To test for isolation by distance, we grouped the ten localities with small sample sizes (< 2) into six groups: (1) Tlatlauquitepec and Las Vigas; (2) Pico de Orizaba and Sierra Negra; (3) Calicanto and Tianguistengo; (4) Volcán Iztaccihuatl; (5) Llano de las Flores and Cumbre Cerro del Cheve; and (6) Cerro Corral del Piedra. For two merged localities into one group, we considered the mid-point coordinates between the two localities as geographical location. We then compared all pairwise geographical distances with all pairwise Wright's inbreeding coefficients (F_{ST}) to test for isolation by distance. All statistics were calculated in R and the F_{ST} statistics were calculated using R software (R Core Development Team) and the R-package adegenet (Jombart, 2008).

Genealogies and networks

We estimated a gene tree for the mtDNA data using maximum likelihood and Bayesian inference. Nucleotide substitution models were selected using JMODELTEST, version 2.1.3 (Darriba *et al.*, 2012). We calculated likelihood scores for 24 candidate models, and used the Bayesian information criterion to select the least parameter-rich model from the 95% credible set of models. Maximum likelihood analyses were conducted using RAxML-VI-HPC, version 7.0.4 (Stamatakis, 2006). The RAxML analyses of the mtDNA data used the GTRGAMMA model of nucleotide substitution. Clade support values were estimated from 100 nonparametric bootstrap replicates. We conducted Bayesian phylogenetic analyses using parallel MrBayes, version 3.1.2 (Ronquist & Huelsenbeck, 2003) with the models selected from JMODELTEST for each codon position. We ran two separate analyses with different starting seeds for 10 million generations using four heated Markov chains (using default heating values). We assessed convergence by comparing the posterior distributions produced by the two separate runs. Posterior probability values were obtained by summarizing the posterior distribution of trees (post burn-in) with a majority-rule consensus tree.

A multilocus network of the nuclear data was used to visualize intraspecific relationships within *S. bicanthalis*. To produce the network, we first calculated uncorrected *p*-distances among alleles at each nuclear locus using PAUP, version 4.0b10 (Swofford, 2003). The genetic distance matrices for separate loci were then combined into a single distance matrix of specimens using POFAD, version 1.03 (Joly & Bruneau, 2006). A genetic network among specimens was constructed using the NeighborNet algorithm (Bryant & Moulton, 2004) in SPLITSTREE, version 4.12.8 (Huson & Bryant, 2006).

Population structure

We inferred population structure using two Bayesian estimation procedures. The first model assumes no admixture so that an individual can only come from any of the K populations. It uses a Dirichlet process prior that infers the assignment of individuals to populations and the number of populations. In the second model, each individual is allowed to have partial ancestry in each of the K populations (admixture) but the number of populations K is fixed. In the second model, the prior distribution for the ancestry of each individual is a Dirichlet distribution. These models were run in STRUCTURAMA, version 2.0 (Huelsenbeck & Andolfatto, 2007). To infer the number of populations using the first model, we performed the analyses using five different priors on the mean number of clusters. Three priors had a mean number of clusters 2, 3, and 4. Additionally, we treated the concentration parameter as hyperparameter and tried two Gamma hyperpriors $G(2,1)$ and $G(0.1,0.1)$ on the concentration parameter.

Species tree and species delimitation

We used the hierarchical Bayesian model implemented in *BEAST, version 1.7.5 (Drummond *et al.*, 2012), to estimate a species tree for the populations of *S. bicanthalis* identified by STRUCTURAMA. *BEAST estimates the species tree directly from the sequence data and incorporates uncertainty associated with gene trees, nucleotide substitution model parameters, and the coalescent process (Heled & Drummond, 2010). Phased nuclear alleles were used in *BEAST analyses, and samples that STRUCTURAMA supported as admixed were removed from the analysis because *BEAST assumes that gene tree discordance arises from incomplete lineage sorting and not gene flow. The analysis took into account the ploidy difference associated with nuclear and mitochondrial genes, and the nucleotide substitution models selected by JMODELTEST were used for each gene partition. A strict clock was applied to each locus, which is a reasonable assumption given the shallow timescale under investigation. We obtained divergence dates on the species tree following the method outlined McCormack *et al.* (2011) by applying a secondary calibration of 5 Mya to the divergence between *S. bicanthalis* and *S. subniger*, a date obtained by a study of the *scalaris* group using three fossil calibrations within *Sceloporus* (Bryson *et al.*, 2012). Uncertainty in this prior knowledge was accommodated using a normal prior probability distribution with a mean ± SD of 5.0 ± 0.5, which resulted in 5% and 95% quantiles at 4 Mya and 6 Mya, respectively. We repeated the analysis twice and Markov chain Monte Carlo (MCMC) analyses were run for a total of 200 million generations (sampling every 10 000 steps and excluding the first 25% as burn-in). We assessed convergence by examining parameter trends between separate runs using TRACER, version 1.5 (Rambaut & Drummond, 2009). Post burn-in samples were combined between the two separate runs and the final posterior distribution of species trees was summarized using a maximum clade credibility tree with median values for node heights.

To investigate whether populations of *S. bicanthalis* might be different species from the perspective of the genetic data, we conducted Bayesian species delimitation using Bayesian Phylogenetics and Phylogeography (BPP, version 2.2; Rannala & Yang, 2013). The model assumes no admixture following speciation and so, as with the species tree analysis, we removed samples that STRUCTURAMA supported as admixed. We ran the rjMCMC analyses for 100 000 generations (sampling interval of 10) with a burn-in period of 1000 generations. We ran each analysis ten times with different starting seeds to check convergence by examining agreement between runs. We used algorithm 0 with the fine-tuning parameter of 2.0. The prior probability for speciation between *S. bicanthalis* and *S. subniger* was set to 1.0 to restrict the rjMCMC analysis from getting trapped on a one-species model that collapsed these two distinct species into one. The prior probabilities for the remaining nodes in the guide tree were set to result in equal prior probabilities for the competing species delimitation models. We evaluated the influence of the priors for population sizes (θ) and the root height of the guide tree (τ) on the posterior probability of species delimitation models by considering different combinations of priors, including large $\theta \sim G(2,10)$ and small $\tau \sim G(2,1000)$, small $\theta \sim G(2,1000)$ and small $\tau \sim G(2,1000)$, and intermediate values for θ and $\tau \sim G(2100)$.

Population size trajectories

A commonly used indicator of genetic diversity within populations is the effective population size. The effective population size is proportional to the rate at which genetic diversity is lost or gained. We took a Bayesian nonparametric approach to estimate changes in effective population sizes by using extended Bayesian skyline plots (EBSP; Heled & Drummond, 2008) for the multilocus data and Bayesian skyride plots (Minin, Bloomquist & Suchard, 2008) for the mtDNA data. Posterior estimates for population size trajectories were obtained using BEAST. For the EBSP analysis, all loci were assigned different substitution models, clock models, and trees using a strategy similar to that used to estimate the species tree. The clock rates for the nuclear genes were assigned a uniform [0,1] prior distribution and estimated relative to the faster evolving mtDNA locus, which was fixed at a substitution rate of 0.02 per million years. This rate comprises an approximation that produced results on the same time scale as the species tree analysis, although it may not be appropriate for obtaining reliable estimates for the timing of population size changes. To quantify the evidence against a constant population size trajectory, we approximated the Bayes factor (B_{10}; Kass & Raftery, 1995) using the MCMC samples to approximate the posterior distribution of a constant population size trajectory (i.e. the proportion of samples with a number of population size changes of zero). The Bayesian skyride analysis utilized the mtDNA data with the same clock model and substitution rate that was used in the EBSP. All analyses were run for a total of 100 million generations (sampling every 100 000 steps and excluding the first 10% as burn-in). We assessed convergence by examining parameter trends between separate runs using TRACER. The Bayesian skyride plot was generated using TRACER, and the EBSP was generated using python scripts supplied on the BEAST website (http://beast.bio.ed.ac.uk).

Population genetic parameter estimates

We estimated population genetic parameters using the multilocus nuclear data, including population sizes (θ), divergence times (τ), and migration rates (m), in a coalescent framework using G-PHOCS, version 1.2.1 (Gronau *et al*., 2011), which is based on BPP software (Rannala & Yang, 2003). Two novel features of G-PHOCS include the modelling of gene flow between populations and the ability to integrate over all possible phase resolutions of genotypic data. We ran ten replicate MCMC analyses for each analysis type with different starting seeds for 400 000 generations (sampling interval of 10) with a 10% burn-in period. The posterior distributions across separate analyses were combined to estimate parameters. The prior probability distributions for $\tau \sim G(2,1000)$ and $\theta \sim G(2,1000)$ matched distributions used in the species delimitation analysis. We assumed that the species tree matched the *BEAST estimate for population relationships: ((north, west), south). Migration rates for the populations that are geographically-adjacent (e.g. north-west and north-south) were estimated using a gamma prior $\sim G(0.002,0.00001)$. The demographic parameters used by G-PHOCS are all scaled by the mutation rate, which requires a conversion to obtain their values in time or number of individuals. We used the divergence time estimated for the root of *S. bicanthalis* from *BEAST to calibrate the population parameters *sensu* Gronau *et al*. (2011). We assumed a generation time of 1.25 years for *S. bicanthalis* based on a demographic study using mark–recapture methods (Rodríguez-Romero *et al*., 2011).

RESULTS

Summary statistics

Among the nine nuclear loci sequenced for *S. bicanthalis*, the genes with the fewest number of variable sites included *BDNF* and *NOS1* (six variable sites each) and *SOCS5* (one variable site), whereas *RAG1* (20 variable sites) and *EXPH5* (23 variable sites) contained the most variation (Table 1). The observed heterozygosity for eight out of nine loci was lower than expected. This difference was significant for seven out of nine loci, indicating that *S. bicanthalis* populations might be inbred. There was no significant linear relationship between F_{ST} values and geographical distance, and therefore we rejected the hypothesis of isolation by distance (Fig. 2).

Genealogies

The mtDNA gene tree based on the complete *ND1* protein-coding gene (972 bp; 67 variable sites) provided strong support for the exclusivity of most sampling localities containing more than one sample (Fig. 1B). Only the southernmost sampling locality (Cerro Corral del Piedra) was not supported as a clade (Fig. 1B). The gene tree was asymmetric with the following branching order of sampling localities (starting at the root): Tlatlauquitepec, Volcán Iztaccihuatl, Pico de Orizaba, Calicanto + Tianguistengo, Las Vigas, Sierra Negra, Llano de las Flores + Cerro Corral del Piedra.

The multilocus network generated using the nine nuclear loci supported two phylogeographical groups within *S. bicanthalis* (Fig. 1C). One of these groups

included samples from the southernmost populations (Cumbre Cerro del Cheve, Llano de las Flores, and Cerro Corral del Piedra), whereas the second group included the remainder of the samples located north of Oaxaca (Fig. 1). The genetic diversity within the southern group was relatively low compared to that of the northern group (Fig. 1C).

Population structure

Bayesian population structure analysis of the nine nuclear loci indicated that $K = 3$ had the highest posterior probability for *S. bicanthalis* (Table 2). This estimate for the number of populations was fairly robust to changes in the type of prior probability distribution used and the parameterization of the prior (Table 2). When the prior probability $E(K) = 4$ was used, the posterior probability for $K = 4$ was highest but only when the dataset was reduced to using only those alleles with ≥ 95% phase confidence. Otherwise, $K = 3$ had the highest posterior probability. The three populations (Fig. 3) were structured as: (1) a southern population located in Oaxaca (Cumbre Cerro del Cheve, Llano de las Flores, and Cerro Corral del Piedra) formed a group that also included a sampling locality in nearby southern Puebla (Sierra Negra); (2) a western population composed of all nine samples from western Puebla (Volcán Iztaccihuatl); and (3) a northern population that includes samples from Puebla (Tlatlauquitepec), Veracruz (Pico de Orizaba and Las Vigas), and Hidalgo (Calicanto and Tianguistengo). Including admixture in the model resulted in several population assignments that introduced mixing between the northern (Pico de Orizaba and Las Vigas) and western (Volcán Iztaccihuatl) populations.

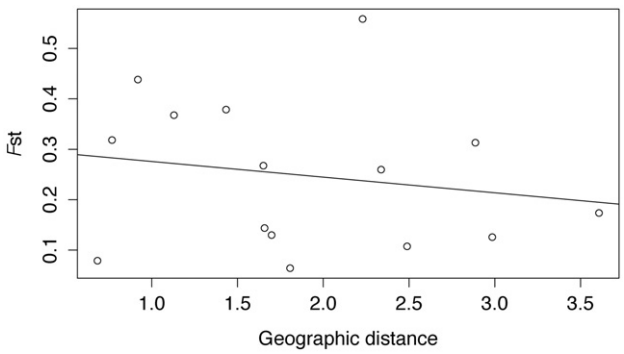

Figure 2. Isolation by distance. Scatter plot comparing genetic and geographical distances using all allele data. All pairwise F_{ST} statistics are used as a measure of genetic distances and Euclidean distances using Global Positioning System coordinates are used as geographical distances. Regression line slope estimated as −0.031 is not significantly different than 0 with *P*-value of 0.51.

Species tree and species delimitation

The two independent *BEAST analyses showed no signs that indicated lack of convergence by 50 million generations, and post burn-in trees were combined to produce a maximum clade credibility tree (Fig. 4). The time-calibrated species tree for the three populations of *S. bicanthalis* supported a sister group relationship (posterior probability = 0.84) between the northern and western populations, and this pairing was sister to the southern population located in Oaxaca and southern Puebla (posterior probability = 1.0; Fig. 4). The timing of divergence within *S. bicanthalis* was recent and did not extend beyond the Middle Pleistocene. The earliest divergence within *S. bicanthalis* that separates the southern population from the others occurred between 308 and 721 kya (mean = 509 kya). Subsequent divergence between the northern and western populations occurred more recently between 198 and 512 kya (mean = 349 kya).

Bayesian species delimitation within *S. bicanthalis* using the nine nuclear loci and mtDNA did not provide strong support for multiple species (Table 3). The prior probability distributions used for population sizes (θ) and root height (τ) had some influence on the posterior distribution of species delimitation

Table 2. Posterior probability distributions for the number of clusters (*K*) in *Sceloporus bicanthalis* using all alleles for the nine nuclear loci

K	*E*(*K*) = 2	*E*(*K*) = 3	*E*(*K*) = 4	Gamma(2,1)	Gamma(0.1,0.1)
1	0.00 (0.00)	0.00 (0.00)	0.00 (0.00)	0.00 (0.00)	0.00 (0.00)
2	0.04 (0.23)	0.01 (0.12)	0.00 (0.05)	0.01 (0.07)	0.03 (0.18)
3	**0.83** (**0.63**)	**0.75** (**0.54**)	**0.66** (0.41)	**0.59** (**0.45**)	**0.72** (**0.52**)
4	0.13 (0.15)	0.23 (0.32)	0.32 (**0.50**)	0.36 (0.05)	0.24 (0.29)
5	0.00 (0.00)	0.01 (0.02)	0.02 (0.04)	0.04 (0.01)	0.00 (0.02)

Posterior distributions for *K* using alleles with ≥ 95% confidence are shown in parentheses. Each column indicates the prior on *K*. The number of populations with the highest posterior probability shown in bold is $K = 3$.

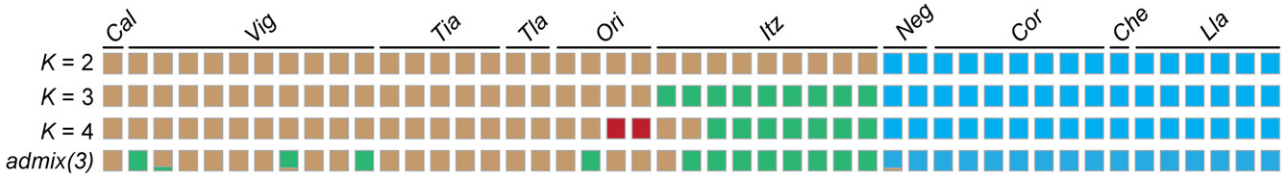

Figure 3. Population structure estimates (mean partitions) for *Sceloporus bicanthalis* based on nine nuclear loci. Each row shows the assignment of individuals to populations (indicated by colour) under a different prior on *K*. The first three rows assume no admixture and fixed values for *K*, and the last row allows admixture (*K* = 3). Cal, Calicanto; Tia, Tianguistengo; Che, Cumbre Cerro del Cheve; Cor, Cerro Corral del Piedra; Lla, Llano de las Flores; Itz, Volcán Iztaccihuatl; Neg, Sierra Negra; Tla, Tlatlauquitepec; Ori, Pico de Orizaba; Vig, Las Vigas.

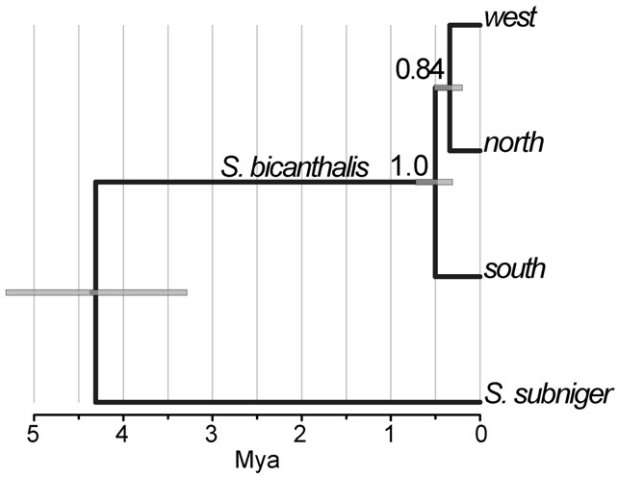

Figure 4. Time calibrated species tree for *Sceloporus bicanthalis* populations. The numbers on nodes are posterior probability values. Grey node bars indicate the 95% highest posterior density for divergence times. Divergence times were estimated using a prior calibration of 5 Mya (±1 Mya; normal distribution) on the divergence between *S. bicanthalis* and *Sceloporus subniger*, a secondary calibration obtained from a study of the *scalaris* group using three fossil calibrations within *Sceloporus* (Bryson *et al.*, 2012).

models, although varying these values by several orders of magnitude did not provide significant results for multiple species. The one-species model received the highest support (posterior probability = 0.694) when using a combination of priors that assumed a large population and shallow divergence, and models with multiple species received low posterior support ≤ 0.17 under these same priors. Posterior support for species delimitation models with two or three species increased when the prior for θ was lower, although the posterior support never exceeded a 0.95 threshold that might indicate a significant result. In addition, Bayes factor tests for alternative species delimitation models only approached a decisive level (Bayes factor = 4.54) for the one-species model (Table 3).

Population size trajectories

Population size trajectories based on all loci (using EBSP) or mtDNA alone (Bayesian skyride) supported a gradual increase through time in population size leading up to the present (Fig. 5). The root of the *S. bicanthalis* lineage was traced back to 500 kya with the population size increase beginning approximately 300–350 kya (Fig. 5); however, this interpretation was contingent on the substitution rate assumption applied to the mtDNA, and changes to that rate will shift the timescale. A slight population size decrease was observed within ≤ 5% of the entire trajectory (Fig. 5). The EBSP analysis also estimated the number of population size changes, and the 95% credible interval for number of changes in *S. bicanthalis* ranged from one to three (median 2; Table 4). The Bayes factor (B_{10}) of 332.6 provides decisive evidence against a constant effective population size trajectory. Conducting separate EBSP analyses for the southern and north + west clade indicated that, even though there is strong evidence against a constant effective population size trajectory in the southern population (Bayes factor of 20.7) and decisive evidence against a constant effective population size trajectory in the north + west clade (Bayes factor of 249), the mean number of population size changes in the southern population is smaller than the north + west population (Table 4).

Population genetic parameter estimates

The migration rates, population sizes, and divergence times for the three populations of *S. bicanthalis* are shown in Table 5. First, the population divergence times were underestimated compared to the *BEAST estimates, although the 95% credible intervals overlapped broadly. The root divergence occurred between 76 and 475 kya (mean = 283 kya), and the divergence between the north and west populations occurred more recently between 198 and 512 kya (mean = 349 kya; Table 5). Second, the population sizes were unequal for the three populations; θ_{north} was approximately twice as large as θ_{west} and almost

Table 3. Bayesian species delimitation in *Sceloporus bicanthalis* provides low support for multiple species

Delimitation model	Prior	$\theta \sim G(2,10)$ $\tau \sim G(2,1000)$	$\theta \sim G(2,1000)$ $\tau \sim G(2,1000)$	$\theta \sim G(2,100)$ $\tau \sim G(2,100)$
One species	0.33	0.694 (4.54)	0.247 (0.73)	0.204 (0.51)
Two species	0.33	0.167 (0.40)	0.497 (1.98)	0.284 (0.79)
Three species	0.33	0.139 (0.32)	0.256 (0.69)	0.512 (2.10)

The Bayes factor for each model is shown in parentheses next to the posterior probability. Posterior probability distributions are means across ten independent runs. Prior distributions for population size (θ) and root height (τ) are shown.

Table 4. The number of population size changes for *Sceloporus bicanthalis* calculated from the extended Bayesian skyline plots

Population	Mean	Median	SE	95% CI lower	95% CI upper	BF_{10}
South	1.64	1	0.105	0	3	20.70
North + west	2.37	2	0.006	1	4	249.0
All	1.81	2	0.101	1	3	332.6

The BF_{10} column provides the Bayes factor to quantify evidence against a constant population size trajectory. CI, confidence interval.

five times larger than θ_{south} (Table 5). The ancestral population sizes reflected the patterns observed in the population size trajectory plots, namely, θ_{root} was 50% smaller compared to $\theta_{north+west}$, which was 20% larger than θ_{north} (Table 5). Finally, migration rates showed a pattern of unidirectional gene flow from the northern population into the western and southern populations. The 95% credible intervals contained zero for all migration estimates, although the posterior means for $m_{north \rightarrow west}$ (mean = 0.272) and $m_{north \rightarrow south}$ (mean = 0.320) were several orders of magnitude higher compared to the reverse migration rates into the peripheral populations ($m_{x \rightarrow north} \geq 0.002$; Table 5).

DISCUSSION

PHYLOGEOGRAPHY OF *S. BICANTHALIS*

Population inferences based on multilocus data suggest that *S. bicanthalis* is composed of three geographically structured populations (Table 2) with minimal genetic exchange between each population (Table 5). The northern and southern populations each contain sampling localities that appear isolated. Conversely, the mtDNA gene tree supports the monophyly of all but one highland population (Fig. 1B), which could be interpreted to support a history of ancient population fragmentation, prolonged isolation, and divergence in allopatry with no gene flow. Interpreting the phylogeographical history of *S. bicanthalis* from the perspective of the mtDNA alone supports the general conclusions made in other highland systems, namely, sky island species typically demonstrate: (1) low genetic diversity within and higher genetic diversity among sky islands; (2) reciprocal monophyly among sky islands; and (3) little to no gene flow among sky islands. These interpretations match the mtDNA patterns found in sky island populations in the Madrean Archipelago, including another species of *Sceloporus* (*Sceloporus virgatus;* Tennessen & Zamudio, 2008), jumping spiders (Masta, 2000), and beetles (Smith & Farrell, 2005), as well as in salamanders in the interior highlands of the USA (Shepard & Burbrink, 2008, 2009). The uniformity in the phylogeographical patterns obtained from these mtDNA studies of sky island species is remarkable; however, the mtDNA gene tree and multilocus history may be at odds, as is the case here with *S. bicanthalis*. It is thus important to acknowledge the boundaries of single-locus inferences and not generalize the pattern found in an mtDNA gene tree to the populations from which they are sampled. Faster sorting times of mtDNA relative to nuclear genes may explain why populations of *S. bicanthalis* are monophyletic. However, because mtDNA is maternally inherited, mtDNA genes only track the history of female dispersal. Male-mediated gene flow that may be important, especially at the population level (Lindell, Méndez-de la Cruz & Murphy, 2008), will be unaccounted for in mtDNA history. Further, gene tree divergences (mtDNA

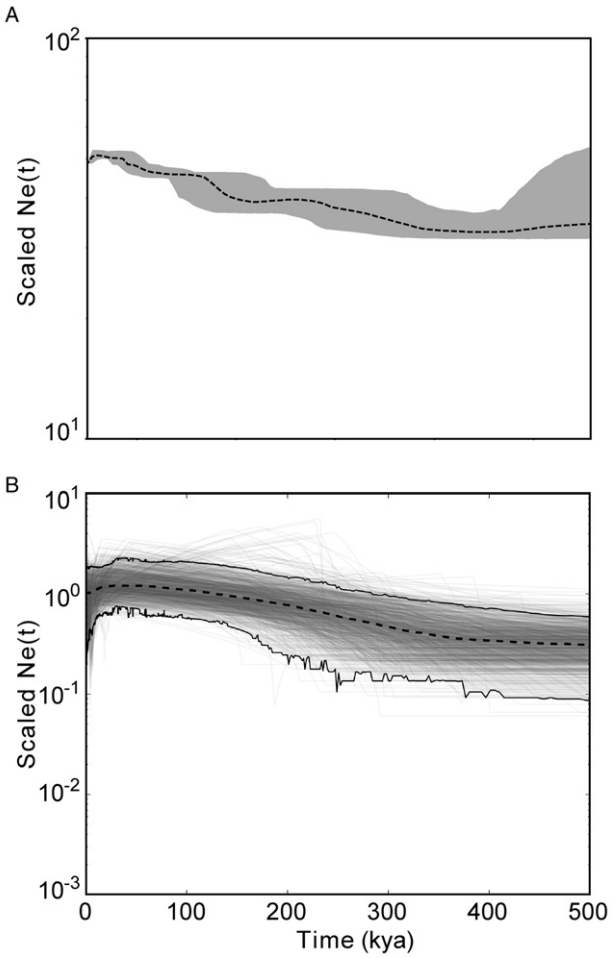

Figure 5. Effective population size trajectories for *Sceloporus bicanthalis*. a, single locus Bayesian skyride analysis using the mitochondrial (mt)DNA data; the median population size is shown with a dashed line, and the 95% credible band is shown in grey. b, multilocus nuclear data and mtDNA analyzed together in an extended Bayesian skyline plot analysis (EBSP); the median population size is shown with a dashed line, the 95% credible band is shown by solid black lines, and each genealogy in the posterior distribution is shown in grey. The *y*-axis is scaled to the product of the effective population size (N_e) and generation time in years.

Table 5. Coalescent-based estimates for population parameters in *Sceloporus bicanthalis*

Parameter	Mean	95% CI lower	95% CI upper
θ_{north}	7096	4564	9754
θ_{west}	3502	1793	5325
θ_{south}	1503	625	2364
$\theta_{north + west}$	8520	1847	15 160
θ_{root}	4323	652	8069
$\tau_{north + west}$	110 794	19 018	304 290
τ_{root}	283 913	76 072	475 453
$m_{west \rightarrow north}$	0.007	0.000	0.102
$m_{north \rightarrow west}$	0.272	0.000	2.383
$m_{south \rightarrow north}$	0.002	0.000	0.028
$m_{north \rightarrow south}$	0.320	0.000	1.875

Posterior probability distributions are means across ten independent runs. Population sizes (θ) are converted to the number of diploid individuals by assuming a mean *S. bicanthalis* divergence of 500 kya and a mean generation time of 1.25 years. The same divergence time is used to convert τ to years. The total migration rate is expressed as the migration rate per generation multiplied by the number of generations spanning the clade. CI, confidence interval.

or otherwise) will necessarily predate species tree divergences. Accordingly, multiple nuclear markers can more robustly estimate demographic histories, gene flow, effective population sizes, and similar population-level processes (Edwards & Bensch, 2009). Multilocus studies are needed to identify any general patterns of population history that are shared among sky island species.

Our multilocus data suggest that *S. bicanthalis* is composed of three populations. We conducted species delimitation model testing to determine whether these three populations represent distinct evolutionary lineages. Species delimitation in this case is essential because the models that we used to calculate population structure do not consider phylogeny and are intended for discerning genetic clusters on much shallower timescales than typical species divergences (Yang & Rannala, 2010). Formulating species delimitation models that contain multiple species and testing them against a single species model is aided by coalescent-based species delimitation (Fujita *et al*., 2012), which provides an objective statistical means for model comparison with the added benefit of phylogenetic underpinnings. That being said, we find low support for species delimitation models that contain multiple species in *S. bicanthalis* using both posterior probability values and Bayes factors (Table 3). Gene flow among populations could bias our inferences since the species delimitation method does not include migration, although under simulation Bayesian species delimitation becomes more conservative and favours fewer species when populations are exchanging genes (Zhang *et al*., 2011). Thus, if migration events were impacting our ability to estimate support for species delimitation models, then we would expect it to reinforce the one-species model. We recommend that *S. bicanthalis* continue to be recognized as a single species, although we note that future research on the

evolution of viviparity in *S. bicanthalis* should not be dissuaded from conducting population comparisons.

Thus far, populations on the western periphery of the species range outside of Mexico City (near Volcán Iztaccihuatl) have been the focus of life history and viviparity research. The populations identified with our current sampling experienced different levels of demographic expansion and size changes, and whether these differences had any lasting impact on the genomic factors underlying viviparity remains an open question. Novel insights into the evolution of viviparity in *S. bicanthalis* could be obtained by contrasting population genomic patterns among the different *S. bicanthalis* populations located across the highlands of south-eastern Mexico.

Phylogeography of regional highland taxa

Our study on the phylogeography of *S. bicanthalis* indicates that Pleistocene climate change had a strong impact on population diversification. Population size changes identified in the EBSP and Bayesian skyride plots (Fig. 5) were probably in response to shifting highland habitats. During cooler Pleistocene glacial cycles, montane vegetation expanded down mountain slopes and linked many previously isolated highland habitats (McDonald, 1993; Marshall & Liebherr, 2000). Subsequently, during warmer interglacial episodes, highland woodlands retracted and their associated biota became isolated (Anducho-Reyes *et al.*, 2008). Population size changes were especially noticeable in the widespread northern population of *S. bicanthalis* (Table 4), consistent with this inference.

Phylogeographical structure in *S. bicanthalis* is broadly similar to that inferred for the montane salamander *Pseudourycea leprosa* (Parra-Olea *et al.*, 2012) and montane rattlesnake *Crotalus intermedius* (Bryson *et al.*, 2011a), indicative of concerted responses to shared historical events. The distribution of *P. leprosa* almost perfectly overlaps the distribution of northern and western populations of *S. bicanthalis*. Within this distribution across the western Trans-Mexican Volcanic Belt, the western populations from Volcán Iztaccihuatl are divergent from the populations to the east in both species, and possibly isolated by the Oriental Basin, a known biogeographical barrier in the region (Bryson *et al.*, 2011b). The distribution of *C. intermedius* ranges from Hidalgo south across the Sierra Madre Oriental into the Sierra Madre del Sur and broadly encompasses the distribution of *S. bicanthalis*. In both *C. intermedius* and *S. bicanthalis*, populations from Oaxaca and southern Puebla (Sierra Negra) form a group that is apparently isolated from populations in Puebla to the north. Although divergences among some populations of *P. leprosa* predated the Pleistocene, most diversification in *P. leprosa*, as well as in *C. intermedius*, was attributable to Pleistocene climate change (Bryson *et al.*, 2011a; Parra-Olea *et al.*, 2012). Considered in concert with similar patterns observed in co-distributed birds (García-Moreno *et al.*, 2004; Puebla-Olivares *et al.*, 2008) and small mammals (León-Paniagua *et al.*, 2007; Hardy *et al.*, 2013), these results suggest that climatic fluctuations during the Pleistocene heavily impacted genetic diversification of montane taxa across south-eastern Mexico.

ACKNOWLEDGEMENTS

The present study would not have been possible without the ample support of the late Fernando Mendoza-Quijano. We also thank O. Flores-Villela and A. Nieto-Montes (MZFC, Universidad Nacional Autónoma de México), I. Solano-Zavaleta, J. L. Aguilar-Lopez, and especially U. O. Garcia-Vázquez for providing tissues; E. Sherman and H. Rockney for help with DNA extraction work at the Burke Museum of Natural History and Culture; and T. Gill for collecting DNA sequences. Collecting in Mexico was conducted under permits granted by SEMARNAT to R. W. Bryson, D. Lazcano, and F. Mendoza-Quijano. We thank two anonymous reviewers for their helpful comments.

REFERENCES

Alföldi J, Di Palma F, Grabherr M, Williams C, Kong L, Mauceli E, Russell P, Lowe CB, Glor RE, Jaffe JD, Ray DA, Boissinot S, Shedlock AM, Botka C, Castoe TA, Colbourne JK, Fujita MK, Moreno RG, ten Hallers BF, Haussler D, Heger A, Heiman D, Janes DE, Johnson J, de Jong PJ, Koriabine MY, Lara M, Novick PA, Organ CL, Peach SE, Poe S, Pollock DD, de Queiroz K, Sanger T, Searle S, Smith JD, Smith Z, Swofford R, Turner-Maier J, Wade J, Young S, Zadissa A, Edwards SV, Glenn TC, Schneider CJ, Losos JB, Lander ES, Breen M, Ponting CP, Lindblad-Toh K. 2011. The genome of the green anole lizard and a comparative analysis with birds and mammals. *Nature* **477:** 587–591.

Andrews RM. 2000. Evolution of viviparity in squamate reptiles (*Sceloporus* spp.): a variant of the cold-climate model. *Journal of Zoology* **250:** 243–253.

Andrews RM, Méndez-De La Cruz FR, Villagrán-Santa Cruz M, Rodríguez-Romero F. 1999. Field and selected body temperatures of the lizard *Sceloporus aeneus* and *Sceloporus bicanthalis*. *Journal of Herpetology* **33:** 93–100.

Anducho-Reyes MA, Cognato AI, Hayes JL, Zuniga G. 2008. Phylogeography of the bark beetle *Dendroctonus mexicanus* Hopkins (Coleoptera: Curculionidae: Scolytinae). *Molecular Phylogenetics and Evolution* **49:** 930–940.

Benabib M, Kjer KM, Sites JW Jr. 1997. Mitochondrial DNA sequence-based phylogeny and the evolution of viviparity in the *Sceloporus scalaris* group (Reptilia, Squamata). *Evolution* **51:** 1262–1275.

Bryant D, Moulton V. 2004. Neighbor-Net: an agglomerative method for the construction of phylogenetic networks. *Molecular Biology and Evolution* **21:** 255–265.

Bryson RW, García-Vázquez U, Riddle B. 2012. Relative roles of Neogene vicariance and Quaternary climate change on the historical diversification of bunchgrass lizards (*Sceloporus scalaris* group) in Mexico. *Molecular Phylogenetics and Evolution* **62:** 447–457.

Bryson RW, Murphy RW, Graham MR, Lathrop A, Lazcano-Villareal D. 2011a. Ephemeral Pleistocene woodlands connect the dots for highland rattlesnakes of the *Crotalus intermedius* group. *Journal of Biogeography* **38:** 2299–2310.

Bryson RW, Murphy RW, Lathrop A, Lazcano-Villareal D. 2011b. Evolutionary drivers of phylogeographical diversity in the highlands of Mexico: a case study of the *Crotalus triseriatus* species group of montane rattlesnakes. *Journal of Biogeography* **38:** 697–710.

Bryson RW Jr, Riddle BR. 2012. Tracing the origins of widespread highland species: a case of *Neogene* diversification across the Mexican sierras in an endemic lizard. *Biological Journal of the Linnean Society* **105:** 382–394.

Creer DA, Kjer KM, Simmons DL. 1997. Phylogenetic relationships of the *Sceloporus scalaris* species group (Squamata). *Journal of Herpetology* **31:** 353–364.

Darriba D, Taboada GL, Doallo R, Posada D. 2012. jModelTest 2: more models, new heuristics and parallel computing. *Nature Methods* **9:** 722–722.

Drummond AJ, Suchard MA, Xie D, Rambaut A. 2012. Bayesian phylogenetics with BEAUti and the BEAST 1.7. *Molecular Biology and Evolution* **29:** 1969–1973.

Edwards S, Bensch S. 2009. Looking forwards or looking backwards in avian phylogeography? A comment on Zink and Barrowclough 2008. *Molecular Ecology* **18:** 2930–2933.

Fujita MK, Leaché AD, Burbrink FT, McGuire JA, Moritz C. 2012. Coalescent-based species delimitation in an integrative taxonomy. *Trends in Ecology & Evolution* **27:** 480–488.

García-Moreno J, Navarro-Sigüenza AG, Peterson AT, Sánchez-González LA. 2004. Genetic variation coincides with geographic structure in the common bush-tanager (*Chlorospingus ophthalmicus*) complex from Mexico. *Molecular Phylogenetics and Evolution* **33:** 186–196.

Gronau I, Hubisz MJ, Gulko B, Danko CG, Siepel A. 2011. Bayesian inference of ancient human demography from individual genome sequences. *Nature Genetics* **43:** 1031–1034.

Grummer JA, Bryson RW Jr, Reeder TW. 2013. Species delimitation using Bayes factors: simulations and application to the *Sceloporus scalaris* species group (Squamata: Phrynosomatidae). *Systematic Biology* (in press).

Guillette LJ Jr. 1982. The evolution of viviparity and placentation in the high elevation, Mexican lizard *Sceloporus aeneus*. *Herpetologica* **38:** 94–103.

Guo SW, Thompson EA. 1992. Performing the exact test of Hardy–Weinerg proportion for multiple alleles. *Biometrics* **48:** 361–372.

Hardy DK, González-cózatl FX, Arellano E, Rogers DS. 2013. Molecular phylogenetics and phylogeographic structure of Sumichrast's harvest mouse (*Reithrodontomys sumichrasti*: Cricetidae) based on mitochondrial and nuclear DNA sequences. *Molecular Phylogenetics and Evolution* **68:** 282–292.

Hedrick PW. 2011. *Genetics of populations*, 4th edn. Sudbury MA: Jones and Bartlett Publishers.

Heled J, Drummond AJ. 2008. Bayesian inference of population size history from multiple loci. *BMC Evolutionary Biology* **8:** 289.

Heled J, Drummond AJ. 2010. Bayesian inference of species trees from multilocus data. *Molecular Biology and Evolution* **27:** 570–580.

Huelsenbeck JP, Andolfatto P. 2007. Inference of population structure under a Dirichlet process model. *Genetics* **175:** 1787–1802.

Huson DH, Bryant D. 2006. Application of phylogenetic networks in evolutionary studies. *Molecular Biology and Evolution* **23:** 254–267.

Joly S, Bruneau A. 2006. Incorporating allelic variation for reconstructing the evolutionary history of organisms from multiple genes: an example from *Rosa* in North America. *Systematic Biology* **55:** 623–636.

Jombart T. 2008. Adegenet: a R package for the multivariate analysis of genetic markers. *Bioinformatics* **24:** 1403–1405.

Kass RE, Raftery AE. 1995. Bayes factors. *Journal of the American Statistical Association* **90:** 773–795.

Leaché AD. 2009. Species tree discordance traces to phylogeographic clade boundaries in North American fence lizards (*Sceloporus*). *Systematic Biology* **58:** 547–559.

Leaché AD, McGuire JA. 2006. Phylogenetic relationships of horned lizards (*Phrynosoma*) based on nuclear and mitochondrial data: evidence for a misleading mitochondrial gene tree. *Molecular Phylogenetics and Evolution* **39:** 628–644.

Leaché AD, Palacios JA, Minin VN, Bryson RW Jr. 2013. Data from: Phylogeography of the Trans-Volcanic bunchgrass lizard (*Sceloporus bicanthalis*) across the highlands of south-eastern Mexico. *Dryad digital repository* doi: 10.5061/dryad.7nv16.

Leaché AD, Reeder TW. 2002. Molecular systematics of the eastern fence lizard (*Sceloporus undulatus*): a comparison of parsimony, likelihood, and Bayesian approaches. *Systematic Biology* **51:** 44–68.

León-Paniagua L, Navarro-Sigüenza AG, Hernández-Baños BE, Morales JC. 2007. Diversification of the arboreal mice of the genus *Habromys* (Rodentia: Cricetidae: Neotominae) in the Mesoamerican highlands. *Molecular Phylogenetics and Evolution* **42:** 653–664.

Lindell J, Méndez-de la Cruz FR, Murphy RW. 2008. Deep biogeographical history and cytonuclear discordance in the black-tailed brush lizard (*Urosaurus nigricaudus*) of Baja California. *Biological Journal of the Linnean Society* **94:** 89–104.

Marshall CJ, Liebherr JK. 2000. Cladistic biogeography of the Mexican transition zone. *Journal of Biogeography* **27:** 203–216.

Masta SE. 2000. Phylogeography of the jumping spider *Habronattus pugillis* (Araneae: Salticidae): recent vicariance of sky island populations? . *Evolution* **54:** 1699–1711.

McCormack JE, Heled J, Delaney KS, Peterson AT, Knowles LL. 2011. Calibrating divergence times on species trees versus gene trees: implications for speciation history of *Aphelocoma* jays. *Evolution* **65:** 184–202.

McCormack JE, Peterson AT, Bonaccorso E, Smith TB. 2008. Speciation in the highlands of Mexico: genetic and phenotypic divergence in the Mexican jay (*Aphelocoma ultramarina*). *Molecular Ecology* **17:** 2505–2521.

McDonald JA. 1993. Phytogeography and history of the alpine–subalpine flora of northeastern Mexico. In: Ramamoorthy TP, Bye R, Lot A, Fa J, eds. *Biological diversity in Mexico: origins and distribution*. 681–703. New York, NY: Oxford University Press.

Mell R. 1929. *Beitrage zur Fauna Sinica. IV. Grundzuge einer ökologie der chinesischen reptilien und einer herpetologischen tiergeographie Chinas*. Berlin: Walter de Gruyter.

Méndez de la Cruz F, Villagrán-Santa Cruz M, Andrews RM. 1998. Evolution of viviparity in the lizard genus *Sceloporus*. *Herpetologica* **54:** 521–532.

Minin VN, Bloomquist EW, Suchard MA. 2008. Smooth skyride through a rough skyline: Bayesian coalescent-based inference of population dynamics. *Molecular Biology and Evolution* **25:** 1459–1471.

Mink DG, Sites JW Jr. 1996. Species limits, phylogenetic relationships, and origins of viviparity in the scalaris complex of the lizard genus *Sceloporus* (Phrynosomatidae: Sauria). *Herpetologica* **52:** 551–571.

Parra-Olea G, Windfield JC, Velo-Antón G, Zamudio KR. 2012. Isolation in habitat refugia promotes rapid diversification in a montane tropical salamander. *Journal of Biogeography* **39:** 353–370.

Portik DM, Wood PL Jr, Grismer JL, Stanley EL, Jackman TR. 2012. Identification of 104 rapidly-evolving nuclear protein-coding markers for amplification across scaled reptiles using genomic resources. *Conservation Genetics Resources* **4:** 1–10.

Puebla-Olivares F, Bonaccorso E, Espinosa de los Monteros A, Omland KE, Llorente-Bousquets JE, Peterson AT, Navarro-Sigüenza AG. 2008. Speciation in the emerald toucanet (*Aulacorhynchus prasinus*) complex. *The Auk* **125:** 39–50.

Rambaut A, Drummond AJ. 2009. *TRACER*, Version 1.5. Oxford: University of Oxford.

Rannala B, Yang Z. 2003. Bayes estimation of species divergence times and ancestral population sizes using DNA sequences from multiple loci. *Genetics* **164:** 1645–1656.

Rannala B, Yang Z. 2013. Improved reversible jump algorithms for Bayesian species delimitation. *Genetics* **194:** 245–253.

Rodríguez-Romero F, Smith GR, Cuellar O, Méndez de la Cruz F. 2004. Reproductive traits of a high elevation viviparous lizard *Sceloporus bicanthalis* (Lacertilia?: Phrynosomatidae) from Mexico. *Journal of Herpetology* **38:** 438–443.

Rodríguez-Romero F, Smith GR, Méndez-Sánchez F, Hernández-Gallegos O, Nava PS, Méndez de la Cruz FR. 2011. Demography of a semelparous, high-elevation population of *Sceloporus bicanthalis* (Lacertilia: Phrynosomatidae) from the Nevado de Toluca volcano, Mexico. *The Southwestern Naturalist* **56:** 71–77.

Ronquist F, Huelsenbeck JP. 2003. MrBayes 3: Bayesian phylogenetic inference under mixed models. *Bioinformatics* **19:** 1572–1574.

Shepard DB, Burbrink FT. 2008. Lineage diversification and historical demography of a sky island salamander, *Plethodon ouachitae*, from the Interior Highlands. *Molecular Ecology* **17:** 5315–5335.

Shepard DB, Burbrink FT. 2009. Phylogeographic and demographic effects of Pleistocene climatic fluctuations in a montane salamander, *Plethodon fourchensis*. *Molecular Ecology* **18:** 2243–2262.

Shine R. 1985. The evolution of viviparity in reptiles: an ecological analysis. *Biology of the Reptilia* **15:** 605–694.

Sinervo B, Méndez de la Cruz F, Miles DB, Heulin B, Bastiaans E, Villagrán-Santa Cruz M, Lara-Resendiz R, Martínez-Méndez N, Calderón-Espinosa ML, Meza-Lázaro RN, Gadsden H, Avila LJ, Morando M, De La Riva IJ, Victoriano Sepulveda P, Rocha CFD, Ibargüengoytía N, Aguilar Puntriano C, Massot M, Lepetz V, Oksanen TA, Chapple DG, Bauer AM, Branch WR, Clobert J, Sites JW Jr. 2010. Erosion of lizard diversity by climate change and altered thermal niches. *Science* **328:** 894–899.

Smith CI, Farrell BD. 2005. Phylogeography of the longhorn cactus beetle *Moneilema appressum* LeConte (Coleoptera: Cerambycidae): was the differentiation of the Madrean sky islands driven by Pleistocene climate changes? *Molecular Ecology* **14:** 3049–3065.

Stamatakis A. 2006. RAxML-VI-HPC: maximum likelihood-based phylogenetic analyses with thousands of taxa and mixed models. *Bioinformatics* **22:** 2688–2690.

Stephens M, Donnelly P. 2003. A comparison of Bayesian methods for haplotype reconstruction from population genotype data. *American Journal of Human Genetics* **73:** 1162–1169.

Stephens M, Smith NJ, Donnelly P. 2001. A new statistical method for haplotype reconstruction from population data. *The American Journal of Human Genetics* **68:** 978–989.

Swofford DL. 2003. *PAUP*. Phylogenetic analysis using parsimony (*and other methods)*, Version 4. Sunderland, MA: Sinauer.

Tennessen JA, Zamudio KR. 2008. Genetic differentiation among mountain island populations of the striped plateau lizard, *Sceloporus virgatus* (Squamata: Phrynosomatidae). *Copeia* **2008:** 558–564.

Tinkle DW, Gibbons JW. 1977. The distribution and evolution of viviparity in reptiles. *Miscellaneous Publications Museum of Zoology, University Of Michigan* **154:** 1–55.

Townsend TM, Alegre RE, Kelley ST, Wiens JJ, Reeder TW. 2008. Rapid development of multiple nuclear loci for

phylogenetic analysis using genomic resources: an example from squamate reptiles. *Molecular Phylogenetics and Evolution* **47:** 129–142.

Townsend TM, Mulcahy DG, Noonan BP, Sites JW Jr, Kuczynski CA, Wiens JA, Reeder TW. 2011. Phylogeny of iguanian lizards inferred from 29 nuclear loci, and a comparison of concatenated and species-tree approaches for an ancient, rapid radiation. *Molecular Phylogenetics and Evolution* **61:** 363–380.

Yang Z, Rannala B. 2010. Bayesian species delimitation using multilocus sequence data. *Proceedings of the National Academy of Sciences of the United States of America* **107:** 9264–9269.

Zhang C, Zhang DX, Zhu T, Yang Z. 2011. Evaluation of a Bayesian coalescent method of species delimitation. *Systematic Biology* **60:** 747–761.

ARCHIVED DATA

DNA sequences are available on GenBank (accession nos.: KF422148–KF422596) and input files for analyses are deposited at Dryad (Leaché *et al*., 2013).

APPENDIX

Locality data and voucher specimen information for all samples used in the present study. Personal field series abbreviations are: FMQ, Fernando Mendoza-Quijano; ISZ, Israel Solano Zavaleta; JLAL, Jose Luis Aguilar Lopez; RWB, Robert W. Bryson Jr.; UOGV, Uri Omar Garcia-Vázquez.

Sceloporus bicanthalis.

HIDALGO: (**Cal**) Calicanto, Hidalgo, MX [20.1561, –98.6808] (FMQ 4200); (**Tia**) Tianguistengo, Hidalgo, MX [20.7854, –98.6611] (FMQ4048, FMQ4096, FMQ4100, FMQ4101, FMQ4103).

OAXACA: (**Che**) Mpo. Santa Maria Papalo, Cumbre Cerro del Cheve, Oaxaca, MX [17.8375, –96.8000] (MZFC13614); (**Cor**) Cerro Corral del Piedra, Oaxaca, MX [17.1696, –96.6571] (FMQ4133-5, RWB7124-7); (**Lla**) Llano de las Flores, Oaxaca, MX [17.4437, –96.5035] (FMQ4124, RWB7110-14).

PUEBLA: (**Itz**) NE slopes of Volcán Iztaccihuatl, Puebla, MX [19.2370, –98.6717] (RWB 7150-3, RWB 7155, RWB 7163, RWB 7165-7); (**Neg**) Sierra Negra, Carr. Vicente Guerrero-Alcomulga, Puebla, MX [18.5016, –97.1860] (UOGV 1198-9); (**Tla**) Tlatlauquitepec, Puebla, MX [19.8544, –97.5041] (ISZ 023, ISZ 207).

VERACRUZ: (**Ori**) Pico de Orizaba, Potrero Nuevo, Veracruz, MX [19.0470, –97.1982] (UOGV 1696, UOGV 1698, UOGV 1701, UOGV 1704); (**Vig**) E Las Vigas, km 125, Veracruz, MX [19.6246, –97.0673] (FMQ 4137-8, FMQ 4141, FMQ 4143-4, RWB 7135-6, RWB 7138-40).

Sceloporus subniger. (outgroup) Mpo. Zacatlan, Piedras Encimadas, Puebla, MX (JLAL 078).